Chapter 4

Studies on porous nanostructured Palladium-Cobalt-Silica as Heterogeneous Catalysts for Oxygen Evolution Reaction

4.1 Introduction

Two major issues that today's globe faces that jeopardise human growth over the long term are the energy crisis and environmental degradation. Exploiting new clean energy sources, such as solar energy, biomass energy, wind energy, and hydrogen energy are major area of study interest in chemistry, energy, and materials science since significant environmental damage typically results from the use of fossil fuels (Ling T et al 2017). The hydrogen energy has received a lot of interest as a high energy density, carbon-free energy source (Fabbri et al 2014 and Viswanathan V et al 2012). An efficient, environmentally friendly, and inexpensive technique of producing a significant amount of H_2 gas is electrochemical water splitting, which uses the cathodic hydrogen evolution reaction (HER) and the anodic oxygen evolution reaction (OER)(Man IC et al 2011). However, during water splitting, the OER, a four-electron transfer mechanism with a high electrode potential, becomes a bottleneck half reaction. Highly active electrocatalysts are thus urgently needed to lower the overpotential and increase the OER rate.RuO_2 and IrO_2 are thought to be the best catalysts for OER due to their high electrocatalytic activity, but due to a number of drawbacks, including high cost, scarcity, and instability, they are not commonly used in the industry (Gerken JB et al 2011, Jiao Y et al 2015, Li X et al 2016 and Song F et al 2018). As a result, one of the research's main

goals continues to be to utilise practical alternative catalysts with affordable prices, enough resources, and effective activity for OER. Since iron, cobalt, and nickel are found in the same section of the periodic table as ruthenium and iridium (group VIII), they naturally get a lot of interest when it comes to catalysts. Transition-metal phosphides(Jin H et al 2015 and Wang J et al 2015), sulphides(Tsutsumi M et al 2017 and Nishioka S et al 2019), selenides(Matsumoto K et al 2021 and P.C.Pandey et al 2014), nitrides(P.C.Pandey et al 2016 and P.C.Pandey et al 2015), borides(P. C. Pandey et al 2018 and P.C.Pandey 2021), and oxides (hydroxides)(Wang B et al 2019, Wang Y et al 2014 and Gao J et al 2018) and many mores(Su J et al 2017, Li CC et al 2010, Zheng F et al 2014, Zheng F et al 2014, Rajabalee FJ et al 1974, Jiang J et al 2017, Guo C et al 2018 and Kumar B, et al 2013) are some cost-effective OER catalysts that have been successfully produced. We have recently described the Synthesis and Properties of Organotrialkoxysilane Functionalized Palladium-Cobalt Heterogeneous Catalysts for Oxygen Evolution (Lee SW et al 2010). Organotrialkoxysilane mediated formation of Co@Pdnps were made using Co-NTA nanowires as a precursor. Three systems of cobalt-palladium nanocatalysts within silica matrix of composition after calcination: (i) Co@Pdnps1 :Si=4.54%; Pd=4.36% and Co=91.10%; (ii) Co@Pdnps2: Si=2.81%; Pd=5.83% and Co=91.36% and (iii) Co@Pdnps3: Si=0.00, Pd=9.48, Co=90.52 are made justifying the impact of nanostructured silica and palladium nano geometry on OER. The presence of nanostructured silica facilitated (a) re-cyclability of nanocatalyst, (ii) significantly improved the palladium nano geometry, (iii) Effective interaction of Cobalt and palladium components during OER. A nanostructured silica-derived thin film composed of Co@Pdnps produced a very high current density at a low overpotential with a minor Tafel slope of 39 mV dec^{-1} and a catalyst loading of 3.5 mg cm^{-2} on the carbon cloth. In the absence of silica, the nanocatalysts are relatively larger with comparatively

less current density(19mAcm^{-2}) as compared to (20.5mAcm^{-2}) recorded with high silica content. One of the major deficiency in this research outcome was related to poor interaction of bimetallic components Since pre-made palladium nanoparticles were mixed with Co@NC into a mortar pestle followed by calcinations at 700^{0}C in an N_2 environment to yield the as reported Co@Pdnps nanocatalyst, ordered organization between palladium and cobalt is not desirable that require in situ interaction during nanoparticles synthesis. However, at high temperatures, Co@NC might have facilitated the interaction between Pdnps and functionalized Co@NC to make nanocomposites as evidenced in the TEM image, which is entirely different from individual TEM images of the nanocomposite's components (Lee SW et al 2010). Accordingly, we attempted herein the formation of in-situ generated Pd-Co bimetallic nanocatalyst in controlled silica matrix allowing the formation of cobalt nanowire in the presence of palladium nanoclusters of variable silica content thus enabling effective interaction of palladium nanoclusters with in-situ generated cobalt nanoparticles. Further, the ratio of organotrialkoxysilane functionalized palladium content along with functional cobalt may further control the silica content; the impact of silica of bimetallic configuration may also be investigated. Such materials may further be calcined to understand the impact of silica on nanogeometry of as generated CoPd@NC since NTA may be transformed during the process causing significant variation of stabilized nanogeometry. Indeed very interesting finding on the formation porous CoPd@NC-1 and CoPd@NC-2 with varying nanostructured silica is recorded and explored in oxygen evolution reactions.Justifying effective bimetallic interaction as evidenced form TEM images as compared to that reported earlier with excellent recyclability for better practical applications.

4.2 Results and Discussion

We recently investigated the role of trialkoxysilane iin making Co-Pd- nanocomposite in silica matrix and studied their role in oxygen evoluition reaction with encouraging findings ((Lee SW et al 2010). The use of NTA as a chelating agent was explored in making Co@NC which was mixed with organotrialkoxysilane derived palladium nanoclusters (Xie Y et al 1990 and Zhang K et al 2016) resulting the formation of Co@Pdnps justifying better OER findings as compared to that of similar finding recorded while using palladium particle of 2 nm size under similar condition ((Lee SW et al 2010). The presence of nanostructured silica caused facilitated OER justifying the novelty on the use of organotrialkoxysilane in deriving nanocatalyst for water splitting reactions (Khan SA et al 2015). One of the major drawbacks of the findings reported recently was mainly concern to the TEM images of Co@Pdnps justifying poor interaction of Co@NC and organotrialkoxysilane derived palladium nanoclusters as the Co@NC was already made and allowed to have specific interaction during calcination processes. Such finding although enabled in proper stabilization of Co nanoparticles however lacked proper geometry of Co-Pd in bimetallic configuration that required further investigation and reported herein. In current investigation cobalt nanowire was initially synthesised in the presence of freshly prepared palladium nanoclusters made from the active role of orgarotrialkoxysilane (Xie Y et al 1990 and Zhang K et al 2016) under hydrothermal process providing seed mediate growth of Cobalt nnanowire under hydrothermal processing along with efficient interaction of palladium nanoclusters with in situ generated Co@NTA creating mesoporous CoPd@NC-1 and CoPd@NC-2. As a result, the initial step is to produce the CoPd-NTA-1 and CoPd-NTA-2, which will be used to fabricate CoPd@NC-1 and CoPd@NC-2. SEM, TEM, and XRD confirm CoPd-NTA production, as illustrated in Figure. Fig.4.1a show SEM pictures of CoPd-NTA-

1,Fig.4.1b show SEM image of CoPd-NTA-2, whereas Fig.4.1c provide x-ray defraction of CoPd-NTA-1 and CoPd-NTA-2, characteristic diffraction peaks of both the Pd and Co crystalline phases were seen in all of the composite's XRD images. The (111), (101), and (130) facets of cubic Pd have diffraction peaks with Bragg angles of 36.78°, 44.76°, and 65.28°, respectively, which have been used to identify the metallic palladium phase (Fig. 1c) (BD-01-088-2335). This observation proves that metallic Pd with afcc structure exists. According to a statement using ICSD database card number 53057, the diffraction peaks appeared at 2Θ values of 18.92°, 31.06°, and 59.19°, respectively, corresponding to the reflection planes (102), (121), and (111).

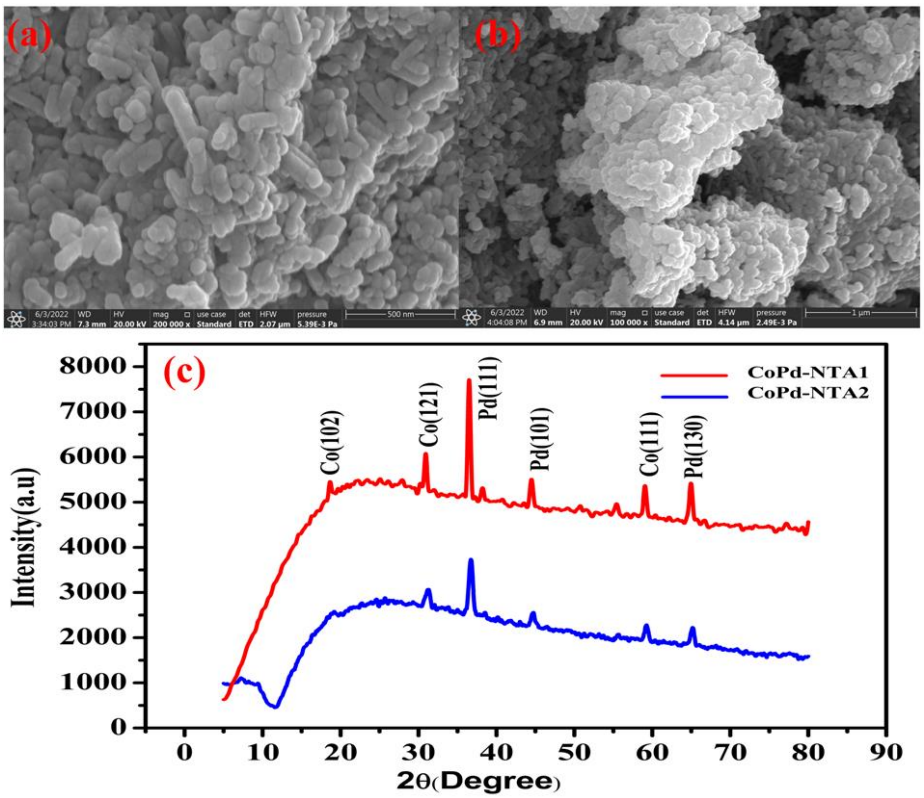

Figure 4.1 SEM image of CoPd-NTA1(a), CoPd-NTA2(b)and X-ray diffraction both CoPd-NTA1, CoPd-NTA2(c), respectively.

This indicates the formation of pure Co in the cubic crystal structure with space group Fm3m.Here the CoPd-NTA-1 and CoPd-NTA-2 indicate that the both of which support

the rod-shaped nano-geometry of the as-made catalyst. The XRD data offered a deeper understanding of the crystalline characteristics of the nanoparticle catalysts Figure 4.2 provide TEM images of CoPd-NTA-1 and CoPd-NTA-2, both of which support the rod-shaped nano-geometry of the as-made catalyst and this results confirm the production of CoPd-NTA-1 and CoPd-NTA-2.

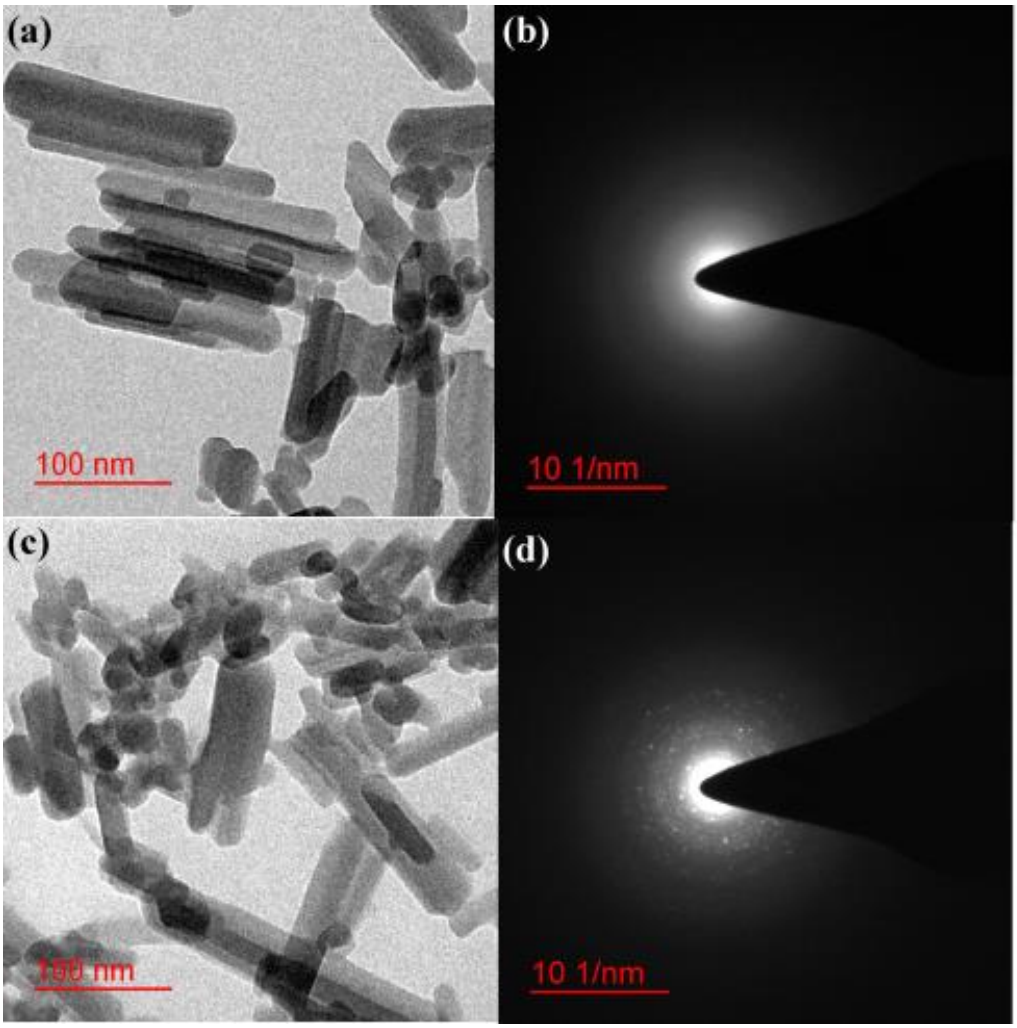

Figure 4.2 TEM images and SAED pattern of CoPd-NTA1 (a),(b) and CoPd-NTA2 (c),(d) respectively.

The next step in the research is the synthesis of CoPd@NC-1 and CoPd@NC-2.Both CoPd-NTA-1 and CoPd-NTA-2 werepyrolyzed at 700^0C for 2 hours to produce CoPd@NC-1 and CoPd@NC-2. TEM, XRD and SEM were used to characterize

CoPd@NC-1 and CoPd@NC-2. In Figure 4.3 the EDX result revealed the creation of CoPd@NC-1 (Fig.3b),the EDX result revealed the creation of CoPd@NC-2 (Fig.3d) and related SEM pictures (Figure 4.3a,c).

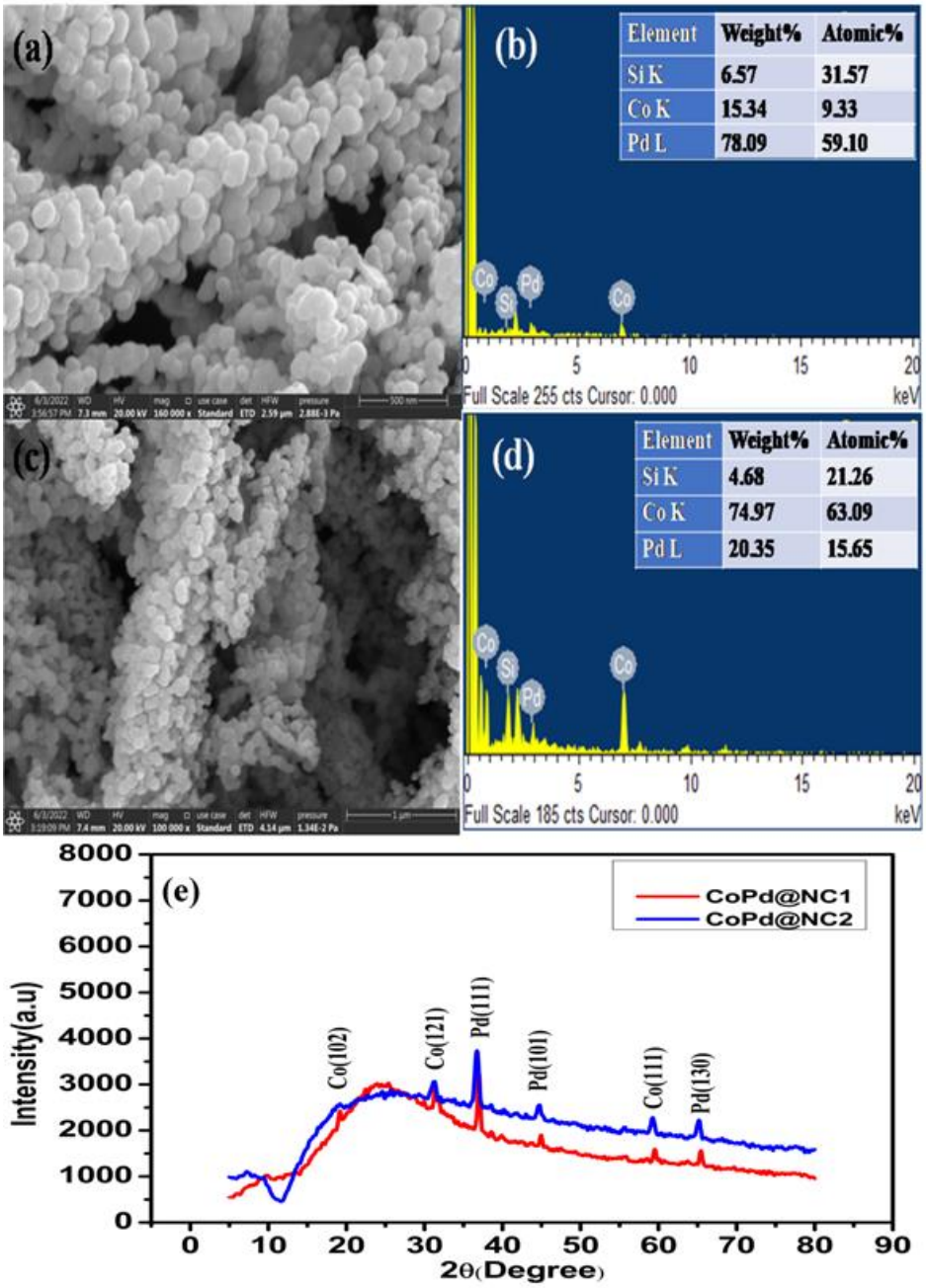

Figure 4.3 SEM image and Energy dispersive x-ray analysis of CoPd@NC-1(a,b), CoPd@NC-2 (b,c) and xrd of both CoPd@NC-1, CoPd@NC-2 (e).

The production of spherical nanoparticles with carbon nanofiber to form one-dimensional growth of the nanostructures by FE-SEM images of CoPd@NC-1 and CoPd@NC-2 as shown in Figure 4.3a,c. The production of CoPd@NC-1 and CoPd@NC-2, which involves the functional activity of different content of silica and chelating cobalt precursors. High-resolution scanning electron microscopy (HR-SEM) was used to examine the shape and size of the as-made nanocatalyst.HR-SEM pictures (Fig.3) at two different magnification reveal the creation of bimetallic CoPd@NC-1 and CoPd@NC-2. In Fig.3b,d the surface atomic ratio of Co to Pd-nanoparticles shows (15.34%Co,6.57%Si,78.09%Pd), which had the higher amount of Si as compared to 3d(74.97% Co, 4.68% Si, and 20.35% Pd) indicating that a Pd shell had covered the Co cores successfully. Figure 4.3-e provide x-ray diffraction of CoPd@NC-1 and CoPd@NC-2,Finally, the production of spherical nanoparticles with carbon nanofiber to form one-dimensional growth of the nanostructures by FE-SEM images of CoPd@NC-1 and CoPd@NC-2 as shown in Figure 4.3a,c. This difference is attributable to the type of electrical distribution used and changes in the two metals' external environments. Figure 4.4a-d shows two different resolutions of TEM images of CoPd@NC-1 and CoPd@NC-2, demonstrating the transformation of Co-rod-shaped NTA morphology to complex morphology. Figure 4.4(b) the selected area electron diffraction (SAED) pattern revealed the crystalline nature of the core. The core-shell structure of the spherical nanoparticles with a Co core wrapped within an N-doped graphene shell was revealed by high-resolution TEM (HRTEM). The core was found to be a mixture of cubic (space group: Fm3m) and hexagonal (space group: P63/mmc) cobalt created by a helpful co-crystallization process. The histogram picture of Pd-nanoparticles in Fig.4c and f, which depicts the size of the CoPd@NC-1 and CoPd@NC-2, demonstrates the relevance of the

amount of alkoxysilane (3-APTMS) in the nanoparticles'-controlled nucleationand the size of CoPd@NC-1 is smaller than the size of CoPd@NC-2.

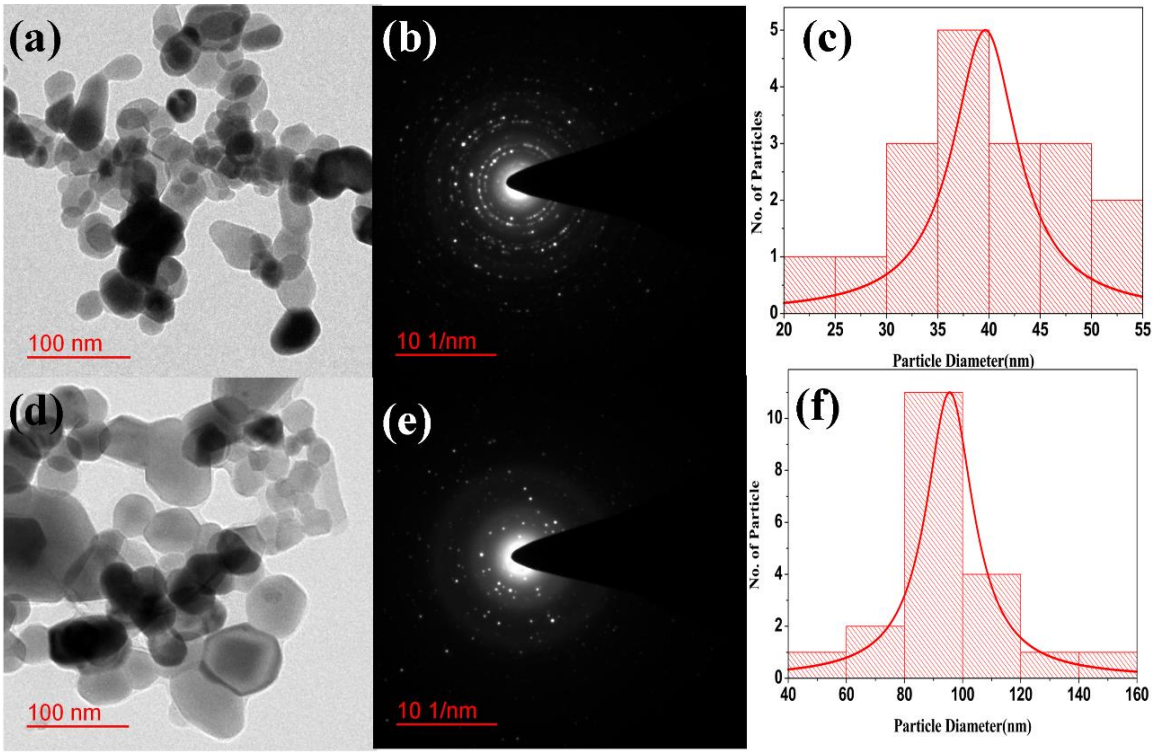

Figure 4.4 TEM images, SAED pattern and particles size distribution of CoPd@NC-1 (a),(b),(c) and CoPd@NC-2 (d),(e), (f), respectively.

N_2 adsorption-desorption isotherms were used to test the porosity of CoPd@NC-1 as seen in Figure 4.5, CoPd@NC-1 exhibited a typical type IV adsorption isotherm. A hysteresis loop can be seen in the graph at P/P0=1-100 because of the mesoporous nature of the CoPd@NC-1. The pore size distribution was depicted as an inset in Figure 4.5 and calculated using the Barrett-Joyner-Halenda [BJH] analytical technique. The CoPd@NC-1 had a limited distribution of pores, and when the pore size was raised up to 100 nm, the pore volume decreased from 0.0045 to 0.001cm^3/g. The specific surface area and total pore volume of the CoPd@NC-1 were estimated using the Brunauer-Emmett-Teller (BET) technique as 50.118m^2/g and 0.002 cm^3/g, respectively.

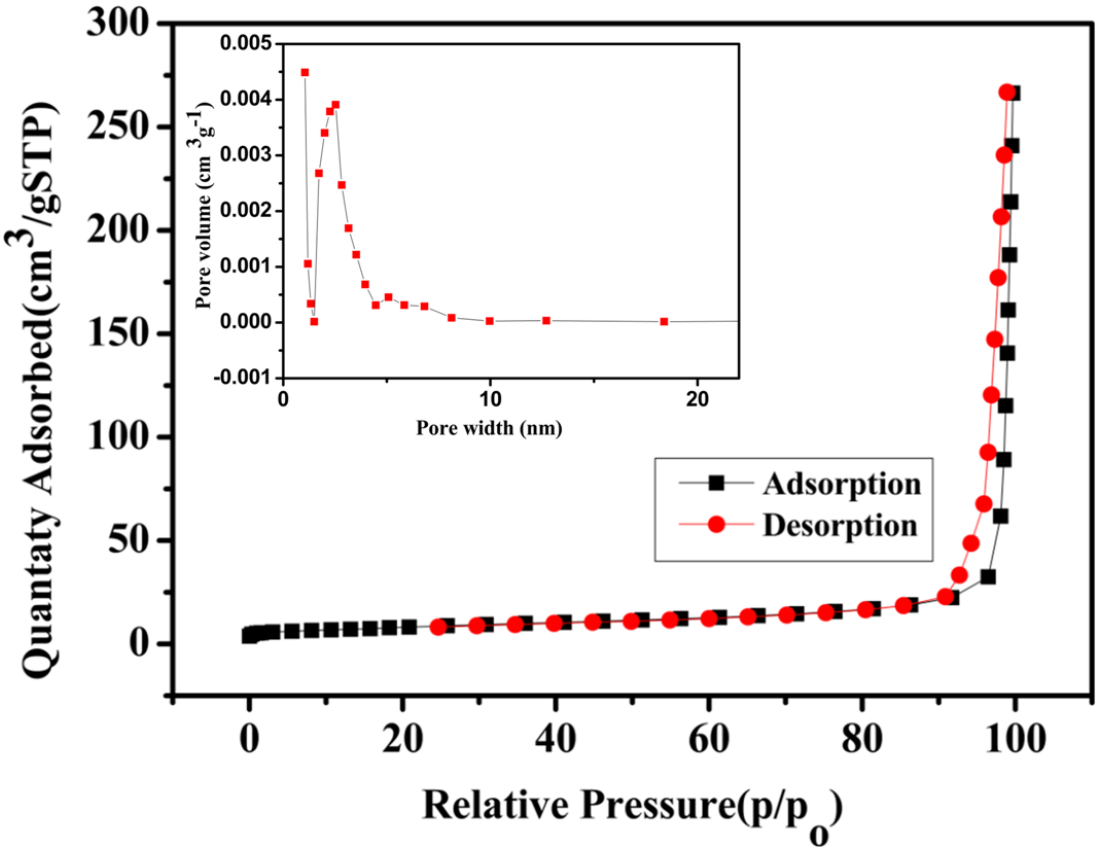

Figure 4.5 N_2 sorption isotherm and pore size distribution (inset) of CoPd@NC-1

4.3 Electrochemistry of Co@NC and CoPd@NC modified electrodes

Effect of nanostructured silica on OER functionalized organotrialkoxysilanes have been used to create CoPd@NC-1, CoPd@NC-2, which were then calcined at 700^0 C to remove the organic functionality link to silica residue. Researchers used linear sweep voltammetry, Tafel plots, electrochemical impedance spectroscopy, and cyclic voltammetry to further understand the oxygen evolution reaction catalysed by Co@NC,CoPd@NC-1 and CoPd@NC-2 modified carbon cloth electrodes, justifying significant advancement as compared to that of Pd-CoOsystem and Co inserted mesoporoussilica (Khan SA et al 2015 and Bikkarolla S et al 2015). Furthermore, the current findings support the first study that developed a powerful and less expensive

bimetallic nanocatalystfor OER, which further supports the function of nanostructured silica dependent OER. Figure 4.6 displays the conclusions on these lines**.**

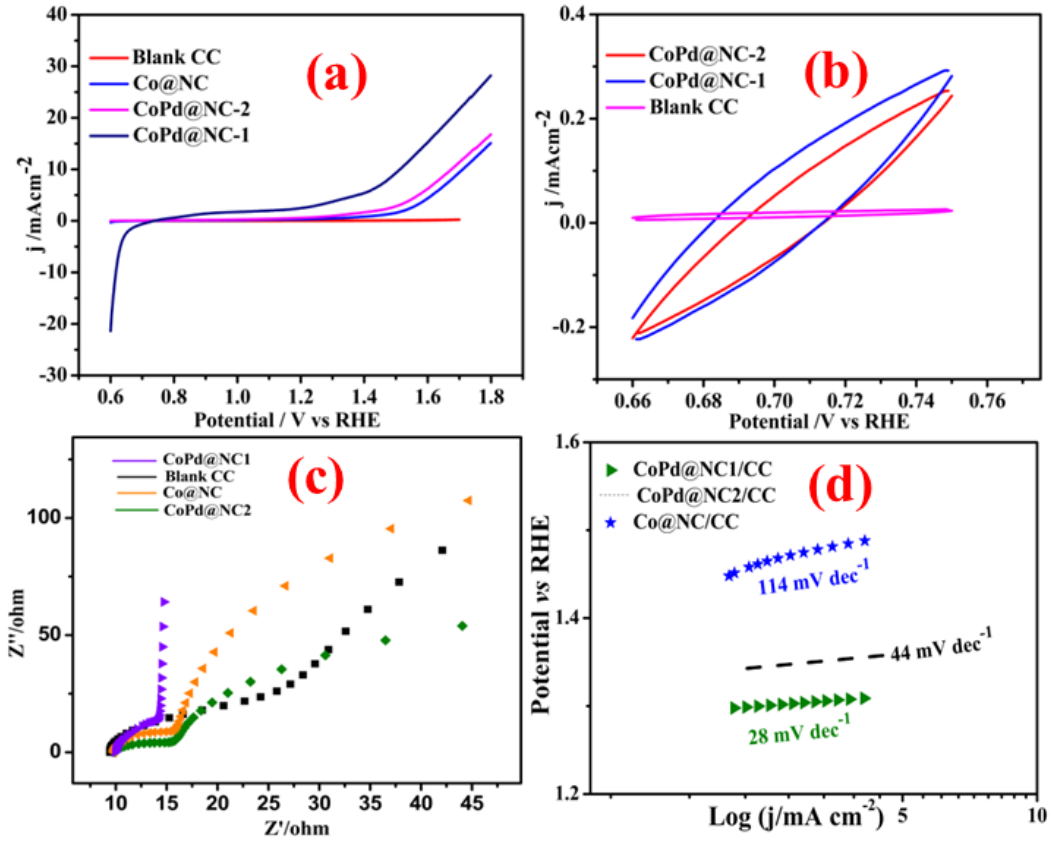

Figure 4.6 Linear sweep voltammetry (a), cyclic voltammetry (b), electrochemical impedance spectroscopy(c), and Tafel plot (d)of bare CC, CoPd@NC-1,CoPd@NC-2,and Co@NC modified electrodes.

Figure 4.6a displays the outcomes of linear sweep voltammetry for unmodified CC, Co@NC, CoPd@NC-1 and CoPd@NC-2 electrodes in 1.0 M KOH solution. The electrocatalytic activity of the raw carbon Cloth for OER was very low. Co@NC,CoPd@NC-1 and CoPd@NC-2, however, enhanced OER, with CoPd@NC-1 displaying significant catalytic activity. The overpotentials for the modified CoPd@NC-1, CoPd@NC-2and Co@NCelectrodes are 0.79 V, 1.29 V and 1.34V respectively, at current densities on the order of $5mAcm^{-2}$.Additionally, the CoPd@NC-1 and

CoPd@NC-2 electrode have a substantially lower overpotential than the Co@NC electrode, demonstrating that the composite material's OER catalytic activity is significantly higher than that of its individual components. Similar findings from cyclic voltammetry of a blank CC, Co@NC, CoPd@NC-1 and CoPd@NC-2 modified electrode are shown in Figure 4.6b. They reveal a several-fold increase in the catalytic activity of CoPd@NC-1whenpalladiumcontent is 2.5mM in the cobalt-based heterogeneous catalyst. The electrochemical impedance spectroscopy (EIS) of a nanocatalyst-modified electrode during production is depicted in Figure 4.6c. The impedance spectra shown in Figure 4.6c have a semicircle part that represents charge transfer resistance and a linear portion that represents diffusion-limited processes. In the instance of Co@NC, the limiting diffusion phase of an electrochemical process was shown by the EIS of the Co@NC-modified electrode (Fig. 4.6), which also showed a long straight line. The electron-transfer resistance (Ret), which is roughly equal to the semicircle diameter, is significantly reduced when 2.5mM palladium is added to a bimetallic heterogeneous catalyst, suggesting a notable increase in catalytic activity for CoPd@NC-1 and CoPd@NC-2 in OER. Supercapacitors have gained a lot of attention as a promising green energy storage technology because of their quick charging and discharging times, high power density, andoutstanding cycle stability. Even though OER and supercapacitors have distinct reaction mechanisms, they both need abundant active sites, strong electrical conductivity, substantial mass transfer, and good electrochemical stability to operate excellently in electrochemistry.The advantages of Co@NC, CoPd@NC-1 and CoPd@NC-2 are demonstrated by the Tafel plot in Figure.4.6d, which supports the low slope value of 28mV/decade. The development of carbon cloth-supported CoPd@NC-1 nanoparticles promotes the electrocatalytic activity of a single component due to the functionality related to the Cobalt precursor and the function of 3-

Aminopropyltrimethoxysilane(3-APTMS) in making heterogeneous catalyst with several folds enhanced catalytic activity in OER. It is essential to understand how well cobalt and palladium nanoparticles placed in a silica matrix work as catalysts. However, after heating the combination to 700°C, the cobalt and palladium components effectively bond with the silica matrix, giving the nanomaterial a high degree of stability. This is followed by tighter contact between the components during catalytic applications. Another important results was recorded justifying sharp increase in current density close to 0.8 V vs NHE revealing potentiality of CoPd@NC-1 in HER which is under investigation in details.

4.4 Conclusions

The recording's outcome reveals the following important discovery, (a)-Polycrystallinity decreases as a function of silica content, and higher nanoparticle geometry is associated with an increase in silica concentration, which enhances the rate of OER, (b)- The variety of polycrystallinity and microstructure of CoPd@NC-1 and CoPd@NC-2 are related to the interaction of various types of silica residue with as-produced Pd. Using a chemical reduction technique, CoPd@NC-1 and CoPd@NC-2Pd-doped bimetallic nanoparticles, were produced following a seed-mediated growth event. Additionally, the ratio of functionalized organotrialkoxysilane palladium to functional cobalt may further regulate the silica concentration, and the effects of bimetallic silica may also be studied. The active activity of organotrialkoxysilane stabilized the nano-size bimetallic nanoparticles, in contrast to other Co@NC catalysts, using a typical example of3-APTMS. The sol-gel method was used to control the nucleation of Pd nanoparticles on cobalt surfaces and promote increased nano geometry during pyrolysis, which led to a several-fold increase in the heterogeneous catalyst's catalytic activity in OER. This was accomplished by

utilizing 3-APTMS steric stabilization capabilities and the sol-gel technique. These nanoparticle catalysts are the most effective bimetallic catalysts for the OER in alkaline conditions, providing a current density of 10 $mAcm^{-2}$at an overpotential of CoPd@NC-1=0.79 V,CoPd@NC-2=1.29V VS NHE and Co@NC=1.34 V at an optimum loading of 3.5 mg/cm^2. Contributions of the chelating CoPd@NC-1 and the silica content to the development of a heterogeneous catalyst for fast OER paved a new way.